Pergamon

Int. J. Impact Engng Vol. 19, No. 4, pp. 331–343, 1997

PII: S0734-743X(96)00041-3
0734-743X/97 $17.00 + 0.00

LOCAL RESPONSE OF CONCRETE SLABS TO LOW VELOCITY MISSILE IMPACT

DAVID Z. YANKELEVSKY

Faculty of Civil Engineering, National Building Research Institute, Technion, Israel Institute of Technology, Haifa 32000, Israel.

(*Received* 15 *April* 1995; *in revised form* 30 *January* and 22 *June* 1996)

Summary—A new model to predict the penetration and perforation of concrete slabs impacted by low velocity missiles, is presented. The two-stage model incorporates a first stage penetration algorithm into an infinite medium and a second stage of punching shear. The transition between stages is determined and the penetration time history as well as concrete plug shear resistance and shape are calculated. The present model predictions are compared with several common formulae as well as with test data and good agreement is obtained. © 1997 Elsevier Science Ltd. All rights reserved.

Key words: concrete, impact, penetration, perforation, punching shear.

INTRODUCTION

Concrete slabs and walls may be required to withstand the effects of missile impact. There exists a variety of potential missiles which differ in their shapes and velocities, such as bullets, fragments, tornado generated missiles, accident generated missiles, etc.

Comparing the relative missile and target deformability, missiles may be classified as either "soft"or "hard". "Soft" missiles deform considerably compared to the target deformation, their response may be uncoupled from the target's response and they are beyond the scope of this work. "Hard" missiles deformation is considerably small compared to the target's deformation and, in many cases, they may be considered as rigid non-deformable missiles. Interest is then focused on target's deformation which is composed of the local damage and the overall response.

The local damage is characterized by the missile penetration into the target, and accompanied effects such as spalling of contrete from the front face of the slab and possible rear face effects. In a relatively thick target no rear face effects will occur, however, when the slab thickness is somewhat decreased, scabbing occurs. When the slab thickness is further decreased, although still larger than the penetration depth of the same missile in a thick target, perforation will occur. Perforation is accompanied with scabbing and shear damage.

The local damage, mainly at about the perforation limit, of a "hard" cylinder, impacting a concrete slab at a low velocity, within the range of 10–200 m/sec, is of our concern in this paper.

Currently the local effects of a "hard" missile impact are determined using empirical formulae [1]. The theoretical attempts to study the problem are limited, as well as their success [2].

The objective of this paper is to provide a theoretical modelling to the perforation mechanism, and to develop an analytical approach for its analysis. In this paper a two-stage penetration–perforation model is presented and comparisons are made with empirical formulae and with test data.

REVIEW OF COMMON PROCEDURES

In this section common procedures for the determination of local effects of penetration and perforation are reviewed. The available methods are empirical or semi-empirical (being based on some theoretical basis), and commonly provide expressions for the maximum penetration depth of an impacting missile which strikes normal to the target, in a thick target,

for the target thickness at which perforation is about to occur (the perforation limit) and for the scabbing limit (which is beyond the scope of this paper). Comprehensive reviews of common methods had been published by several authors. This section includes a review of classical empirical formulae, which are extracted from the comprehensive review presented by Kennedy [1], as well as presentation of several more recent expressions. These empirical and semi-empirical expressions provide a basis for comparisons with the present model predictions in subsequent sections.

The modified Petry formula

The penetration depth x (inch) in a thick concrete target is given by:

$$X = 12\, K_p\, A_p \log_{10}\left(1 + \frac{V_0^2}{215000}\right). \tag{1}$$

The form of this expression results from the solution of the equation of motion in which the instantaneous resisting force is expressed by a constant term and a drag resisting component depending on the striking velocity V_0 (fps) squared. A_p is the missile section pressure, expressed as its weight per unit area (1bs/ft^2).

K_p is a material coefficient which originally was dependent on how the concrete is reinforced (e.g. $K_p = 0.00426$ for normal reinforced contrete), and was modified to consider concrete strength [3]. Thus, in the modified Petry formula $K_p = 0.0035$ for concrete strength of 3000 psi. The original presentation was denoted by Kennedy as "modified Petry I", and the modified presentation as "modified Petry II".

Amirikian suggested that the perforation thickness be given by:

$$e = 2x. \tag{2}$$

The Army Corps of Engineers formula

The penetration depth in a thick concrete target is given by the empirical formula:

$$\left(\frac{x}{d}\right) = \frac{282\, D d^{0.215}}{(f'_c)^{1/2}}\left(\frac{V_0}{1000}\right)^{1.5} + 0.5 \tag{3}$$

where d is the missile diameter (in), D is the missile caliber density W/d^3 (lbs/in^3) and f'_c is the ultimate concrete compressive strength (psi).

The perforation thickness is given by

$$\frac{e}{d} = 1.32 + 1.24\left(\frac{x}{d}\right) \quad 3 \le \frac{e}{d} \le 18. \tag{4}$$

The modified NDRC formula

The National Defense Research Committee developed a penetration theory which yielded the expression for the penetration depth in a thick target:

$$G\left(\frac{x}{d}\right) = K N d^{0.20} D\left(\frac{V_0}{1000}\right)^{1.8} \tag{5}$$

where

$$G\left(\frac{x}{d}\right) = \begin{cases} \left(\dfrac{x}{2d}\right)^2 & \text{for } \dfrac{x}{d} \le 2.0 \\ \left[\left(\dfrac{x}{d}\right) - 1\right] & \text{for } \dfrac{x}{d} \ge 2.0. \end{cases} \tag{5a}$$

N is the nose shape factor (e.g. $N = 0.72$ for a flat nose and 1.00 for average bullet nose); K is a parameter of concrete strength, which is given by Kennedy:

$$K = 180/(f'_c)^{1/2}. \tag{5b}$$

For large slab thickness to missile diameter ratios the perforation slab thickness will be calculated according to Eqn (4). For small ratios another expression had been proposed:

$$\frac{e}{d} = 3.19\left(\frac{x}{d}\right) - 0.718\left(\frac{x}{d}\right)^2 \quad \text{for} \quad \frac{x}{d} \leq 1.35. \tag{6}$$

The Ballistic Research Laboratory formula

An expression which directly calculates the perforation thickness had been suggested by the BRL:

$$\frac{e}{d} = \frac{427}{(f'_c)^{1/2}} D d^{0.2} \left(\frac{V_0}{1000}\right)^{1.33}. \tag{7}$$

The Ammann and Whitney formula

This formula had been proposed to predict the penetration of small explosively generated fragments at relatively high velocities:

$$\left(\frac{x}{d}\right) = \frac{282 N D d^{0.2}}{(f'_c)^{1/2}} \left(\frac{V_0}{1000}\right)^{1.8}. \tag{8}$$

The Haldar formula

Haldar introduced a dimensionless parameter I, called the impact factor [4]:

$$I = \frac{WNV^2}{gd^3 f'_c}. \tag{9}$$

All the parameters in Eqn (9) are identical to the parameters in the NDRC equations.

Correlation of penetration test results with the impact factor yielded the following expressions for penetration depth prediction:

$$\frac{x}{d} = -0.0308 + 0.25251\text{I} \quad 0.3 \leq I \leq 4 \tag{10a}$$

$$\frac{x}{d} = 0.6740 + 0.567\text{I} \quad 4 < I \leq 21 \tag{10b}$$

$$\frac{x}{d} = 1.1875 + 0.0299\text{I} \quad 21 < I \leq 455. \tag{10c}$$

Scabbing and perforation are calculated using NDRC formulae.

The Kar formula

Kar developed the following empirical formulae utilizing regression analysis [5]:

$$G\left(\frac{x}{d}\right) = \frac{180}{(f'_c)^{0.5}} N_2 \left(\frac{E}{E_m}\right)^{1.25} \frac{W}{D.d^{1.8}} \left(\frac{V}{1000}\right)^{1.8} \tag{11}$$

where N_2 = nose shape factor, and E, E_m = elasticity moduli of the target and the missile, respectively.

The penetration depth x is determined from Eqns (12a) and (12b):

$$G\left(\frac{x}{d}\right)=\begin{cases}\left(\dfrac{x}{2d}\right)^2 & \text{for} \quad \dfrac{x}{d}\leq 2 \qquad (12a)\\[2ex] \left(\dfrac{x}{d}-1\right) & \text{for} \quad \dfrac{x}{d}\geq 2. \qquad (12b)\end{cases}$$

The depth e to prevent perforation is:

$$\frac{e-a}{d}=3.19\frac{x}{c}-0.718\left(\frac{x}{c}\right)^2 \quad \text{for} \quad \frac{x}{d}\leq 1.35 \qquad (13a)$$

$$\frac{e-a}{d}=1.32+1.24\left(\frac{x}{d}\right) \quad \text{for} \quad 3\leq\frac{e}{d}\leq 18 \qquad (13b)$$

where a is half the aggregate size in concrete.

The UKAEA formula

Based on extensive studies the U.K. Atomic Energy Authority recommended techniques to predict the penetration and perforation thickness [6].

The normalized penetration depth z can be estimated from the formulae:

$$G=\frac{3.8\times 10^{-5}NmV_i^{1.8}}{f_c^{0.5}d^{2.8}} \qquad (14)$$

$$G=0.55z-z^2 \quad \text{for} \quad z=\frac{x}{d}<0.22 \qquad (15a)$$

$$G=\left(\frac{z}{2}\right)^2+0.0605 \quad \text{for} \quad 0.22<z<2 \qquad (15b)$$

$$G=z-0.9395 \quad \text{for} \quad z>2. \qquad (15c)$$

The perforation velocity V_c is:

$$V_c=1.3\rho^{1/6}f_c^{1/2}\left(\frac{pe^2}{\pi m}\right)^{2/3}(r+0.3)^{1/2} \qquad (16)$$

where

ρ = concrete density (kg/m^3),
p = missile perimeter (m),
d = missile diameter (m),
e = concrete thickness (m),
m = missile mass (kg),
r = reinforcement quantity (%) and,
f_c = ultimate compressive strength of concrete (P_a)

All the available methods provide calculation tools, most of which are based on curve fitting to test data. Comparison of available test data with these methods will be discussed later.

A MODEL FOR LOW VELOCITY PENETRATION AND PERFORATION

General description

A relatively simple model is proposed to describe the penetration and perforation mechanism of a missile in a concrete slab. The process is modelled by two interconnected

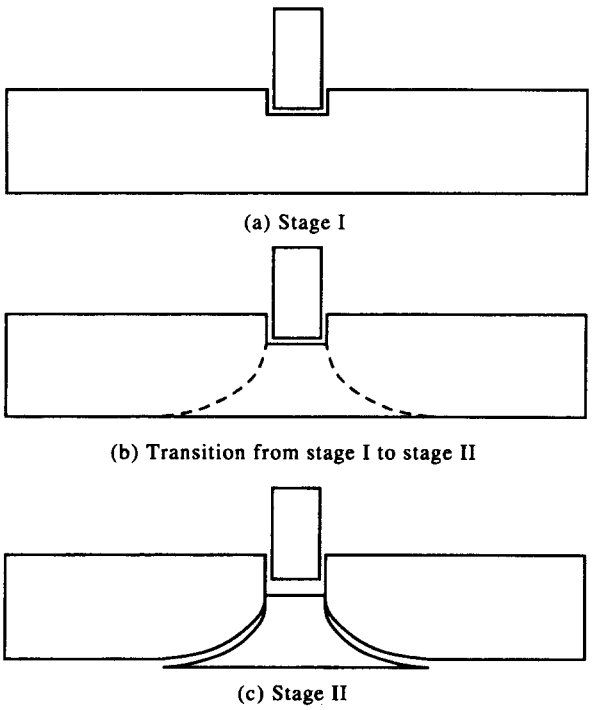

Fig. 1. A two-stage penetration model.

stages. In the first stage [Fig. 1(a)] the missile penetrates a semi-infinite medium where no effect of the rear slab face affect the penetration process. When the plastic shock front ahead of the missile, which carries a considerably larger amount of energy than the elastic wave ahead of it, meets with the rear boundary, curved shear cracks are developed and a bell-shaped plug is formed [Fig. 1(b)]. In the second state [Fig. 1(c)] the missile pushes the plug, shears it off the surrounding concrete and continues penetrating through it. The perforation thickness is then the thickness required to penetrate and completely shear off the plug, and bring to a complete stop the missile and the plug at the end of this process.

Stage I—dynamic penetration

In the first stage of discs model, which had earlier been developed by the author [7], has been adopted. In this model the target is subdivided into a set of discs having a common axis of symmetry (Fig. 2). The response of a typical disc in its plane is intitiated once the missile nose meets the discs level. The nose creates a hole, the instantaneous radius of which depends on the local nose shape. In the case of a flat nose, the target material in front of it is compressed, thus forming a forged nose which travels ahead of the missile and its shape is close to a cone. The one-dimensional equation of motion of a typical disc, in Lagrangian cylindrical coordinates (Fig. 3), is:

$$\rho_0 r\ddot{u} = -(r+u)\frac{\partial \sigma_r}{\partial r} - (\sigma_r - \sigma_\theta)\frac{\partial (r+u)}{\partial r} \tag{17}$$

where ρ_0 is the initial mass density, r is the Langrangian coordinate, u is the radial displacement, σ_r, σ_θ are the radial and tangential stresses, respectively.

The conservation of mass requirement yields:

$$\frac{\rho_0}{\rho} r = (r+u)\frac{\partial (r+u)}{\partial r} \tag{18}$$

where ρ is the current mass density.

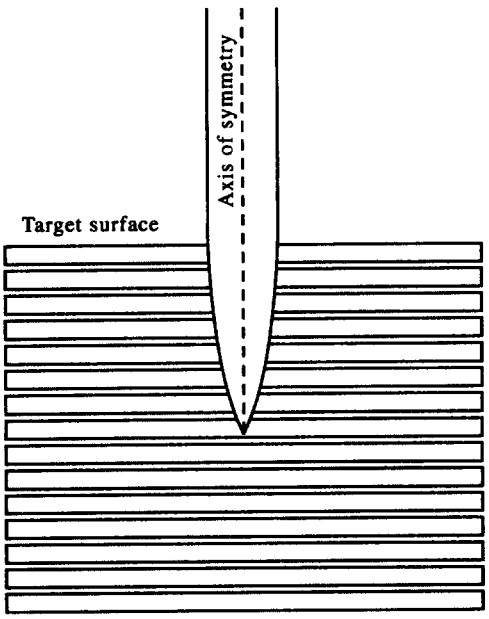

Fig. 2. Discs model for first stage penetration.

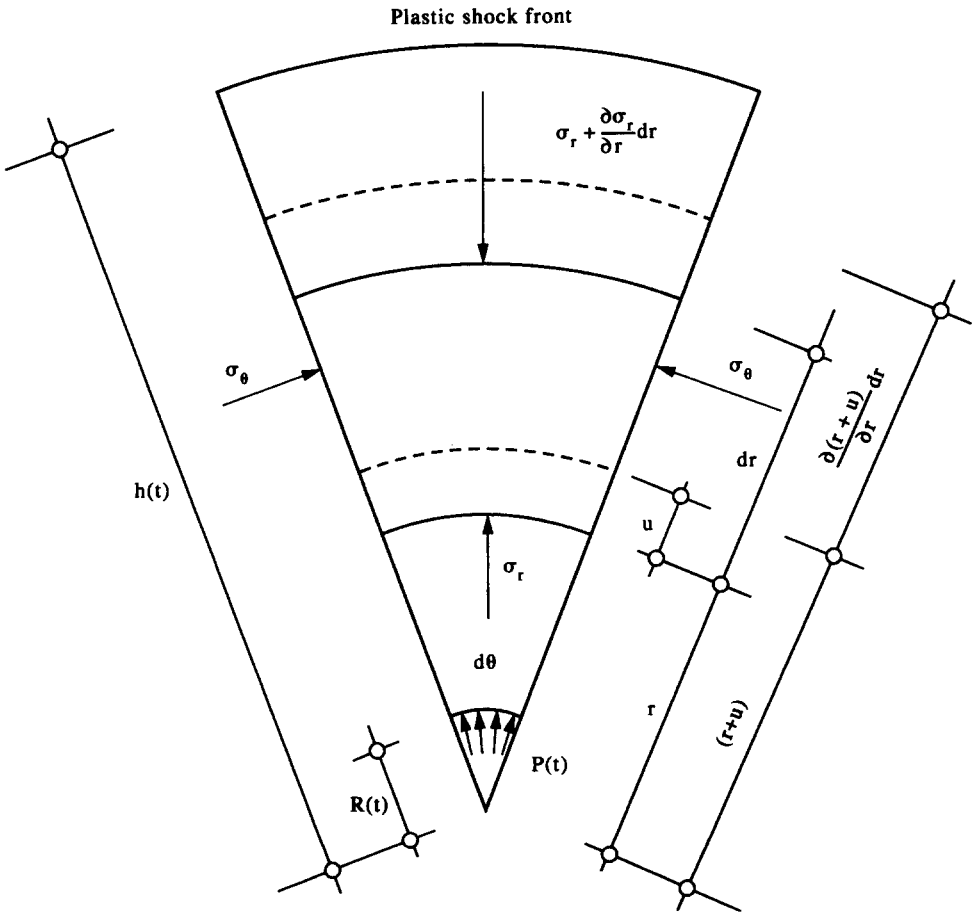

Fig. 3. Sector of a typical disc.

The principal governing mechanism is assumed to be high local volume changes as a result of plastic deformations, and elastic deformations had been ignored. To simplify the mathematical derivation, the constitutive equations had been simplified, the hydrostatic component was represented by a locking model, assuming that the medium locks behind the plastic shock front at a volumetric strain ε_L, and the principal stress difference at failure is assumed to have a constant value. However, to better represent the real constitutive relationships in concrete, where the volumetric strain and the principal stress difference at failure depend on the magnitude of the hydrostatic stress, a floating locking behavior had been defined in which the locking volumetric strain magnitude is determined to represent an average magnitude of the hydrostatic stress in the plastic zone of the stressed disc. The locking strain magnitude is obtained by equating the virtual work done on strain increments by the variable stresses in the plastic zone and the components of the average hydrostatic stress:

$$\int_v \sigma_r \dot{\varepsilon}_r \, dV + \int_v \sigma_\theta \dot{\varepsilon}_\theta \, dV = \bar{\sigma}_r \int_v \dot{\varepsilon}_r \, dV + \bar{\sigma}_\theta \int_v \dot{\varepsilon}_\theta \, dV \tag{19}$$

where $\dot{\varepsilon}_r, \dot{\varepsilon}_\theta$ are radial and tangential strain increments, respectively, σ_r, σ_θ are variable radial and tangential stresses, respectively, and $\bar{\sigma}_r, \bar{\sigma}_\theta$ are radial and tangential components of the average hydrostatic stress.

Thus, a variable locking strain is obtained, which corresponds to the average hydrostatic stress level, and the "constant" value of the principal stress difference at failure is determined to correspond to this stress level as well.

Using the above equations and the Rankine–Hugoniot jump conditions at the shock front, yields the expression for the interaction pressure on the internal boundary of the disc, which equals in magnitude to the horizontal component of the target instantaneous resisting force at this level. The resisting force at any instant is found.

This procedure is formulated in a computer program which calculates the missile motion and the target response at all times.

Stage II—plug formation and shear

Consider a concrete slab of thickness H, through which a missile had penetrated to a certain depth and pressure is exerted at a contact area, in an attempt to shear off the remaining thickness h (Fig. 4). At the short time durations considered, global response of the target is negligible, and plug shear may be assumed as a relative displacement of a rigid plug with respect to its rigid surroundings. Since the cracked surfaces are rough, shear and normal stresses are developed due to aggregate interlock, depending on the crack width and its shear displacement. These values, in turn, depend on the relative displacement in the direction of motion and on the crack geometry. The contribution of reinforcement has not yet been incorporated in the model and resistance is due to concrete shear only. Examination of the mode of deformation of the plug with respect to the target, indicates that the reinforcement is not likely to have a significant contribution to the resistance, because the plug pushes ahead the reinforcing bars at the targets backface, which are peeled off through the thin concrete cover. Reinforcements contribution is increased when precautions are taken to prevent low resistance mode of peeling off failure, and this case is beyond the scope of the present model. Thus, although the model is formulated to predict unreinforced targets behavior, its prediction of normally reinforced concrete targets may be reasonable. Since this study is limited to low velocity impact, it is assumed, at this stage, that the static values govern, and strain rate effects may be disregarded. Thus, for a variable yet unknown, shape of the plug $r(x)$, one may determine the displacement components along the crack and the corresponding stresses [8]. Integrating the contributions of the variable shear and normal stresses along the cracked surface for a given relative displacement, yields the total resisting force:

$$P(u) = 2\pi \int_0^h \left[\tau(u) - \sigma(u) \frac{dr(x)}{dx} \right] r(x) dx. \tag{20}$$

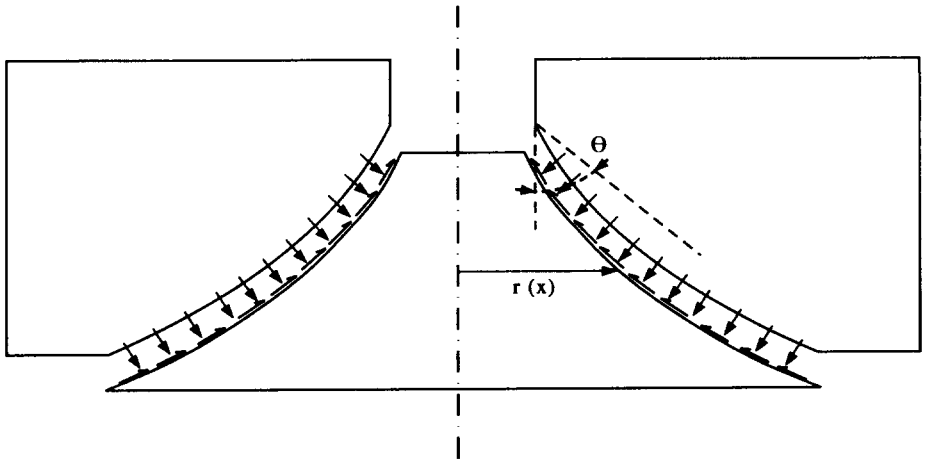

Fig. 4. Punching shear in the second stage.

A minimization algorithm determines the shape of the plus $r(x)$, which, among all possibilities, yields the minimum resisting force, and for this shape the complete resisting force vs relative displacement may be calculated (Fig. 5). On these grounds one may determine the energy dissipated in the plug complete shear off the slab. This procedure had been adopted to study problems of punching shear in concrete and very good predictions were obtained.

Transition from Stage I to Stage II

The total resisting force in Eqn (20) depends on the remaining thickness h, which has not yet been determined. The larger the thickness h, the greater the resisting force P [Eqn (20)] and its peak value. The missile continues to penetrate the target until it reaches a depth X_1 [Fig. 1(b)]. At this depth the instantaneous resisting force to its motion equals the peak force which is required to shear off the remaining plug. At a smaller penetration depth the force which resists the missile motion is smaller than the plug shear resistance, and this mechanism cannot be activated. The condition which determines whether the plug will completely be sheared off is the requirement that the missile remaining kinetic energy be equal to the total dissipation energy in a complete plug shear.

At stage II the projectile penetrates into the plug and at the same time the plug is pushed outside relative to the rest of the target. The two simultaneous motions are interconnected through the interaction force R_2 (Fig. 6).

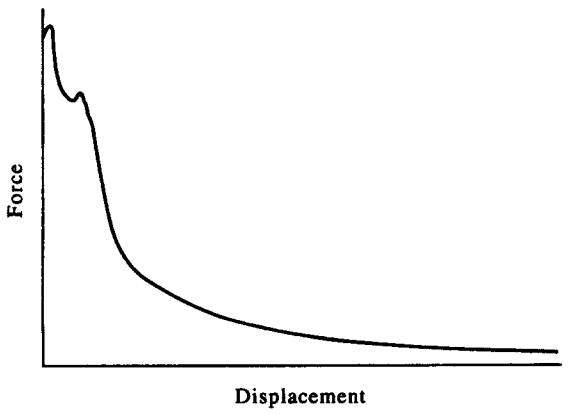

Fig. 5. Force–displacement relationship in punching shear.

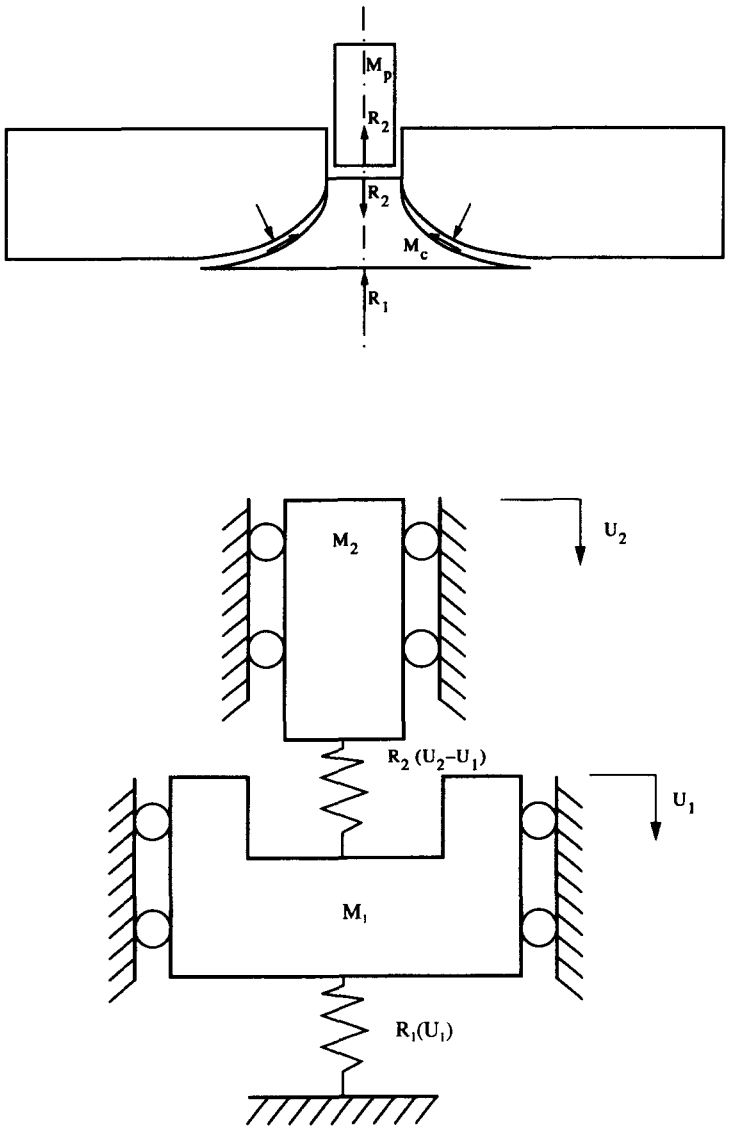

Fig. 6. Transition from the first stage to the second stage.

Example 1: comparison with empirical formulae

Kennedy presents a comparison between several empirical formulae in predicting the penetration depth in a thick target and the perforation thickness [1]. The missile weighs 45.45 kg, its diameter is 15.24 cm, and its nose shape factor is $N = 1$.

Figure 7 shows the calculated penetration depths according to these formulae and, according to the proposed penetration model, this governs the missile's motion in phase I. The proposed model follows closely the modified NDRC equations within the range of 0–300 m/sec. The calculated perforation thickness is shown in Fig. 8. Several points were calculated and it was found that, at higher impact velocities, the deceleration level elevates and the resisting force increases. Therefore, h increases with increase of the impact velocity. This is probably the reason for the multiplier of x in Eqns (4) and (6).

Example 2: tests at AEE Winfrith and at Meppen

A full size test of a flat faced right cylinder rigid missile had been conducted at the Bundeswehr experimental establishment, Meppen, and models at two scales were tested at

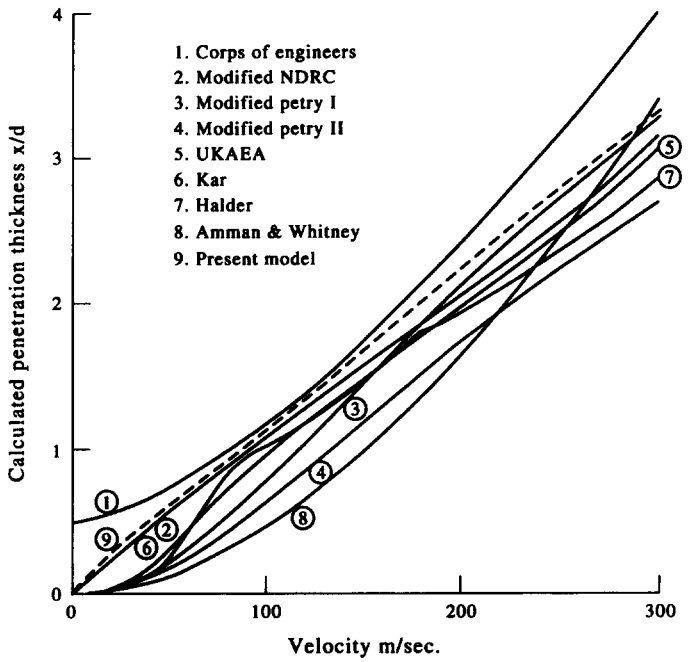

Fig. 7. Example 1—calculated penetration depth.

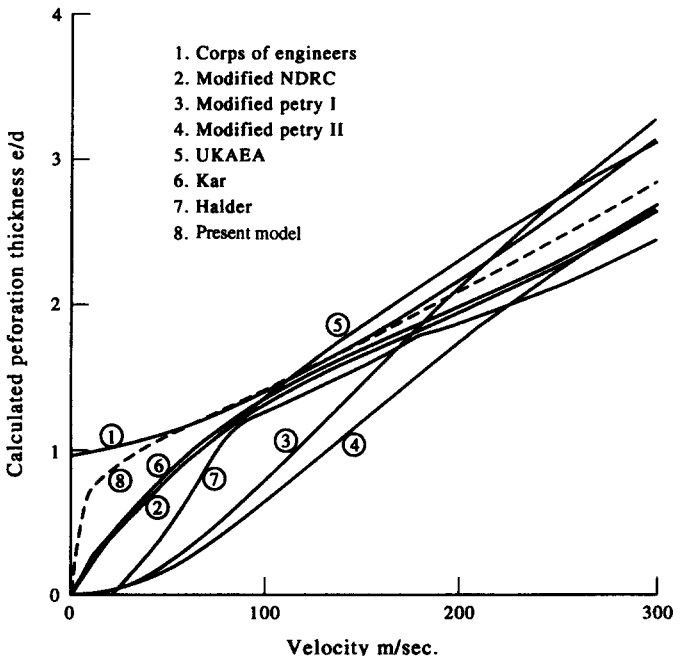

Fig. 8. Example 1—calculated perforation thickness.

AEE Winfrith [9]. Details of the target and missile data are given in Table 1. Concrete strength in the various targets varied between 30–40 MPa.

The impact velocity in the Meppen test was 76 m/sec, and was assumed to be very close to the velocity needed just to achieve perforation. A similar velocity had been determined as the perforation limit velocity for the smaller scale targets. Comparison with the proposed model has been performed with the small scale target, to which data is provided, describing the cross-section of the perforated plate [Fig. 9(a)]. Calculations with the proposed model

Table 1. AEE Winfrith and Mappen tests

Target		Missile	
Diameter (m)	Thickness (m)	Mass (kg)	Diameter (m)
6.0	0.640	475	0.312
2.3	0.246	27	0.120
0.767	0.082	1	0.040

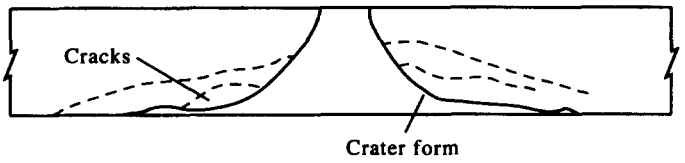

(a) Crater form – Experiment

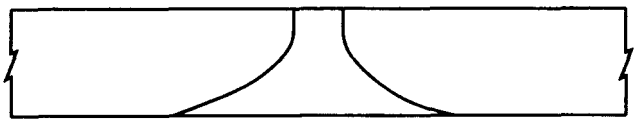

(a) Crater form – Analytical model

Fig. 9. Example 2—comparison of experimental perforation results with models prediction.

predict perforation, and the theoretical cross-section of the perforated target is shown in Fig. 9(b).

Example 3: SRI tests

Several tests had been carried out at SRI [2] in which flat nosed projectiles, 22 mm in diameter, were shot towards 50 mm thick reinforced concrete targets, at different velocities. Table 2 summarizes the results of four tests and the predicted penetration depth of three common empirical formulae. In Table 3 the perforation limit thickness corresponding to each of the impact velocity levels, is shown, being calculated using three different equations.

The calculated results indicate that, for an impact velocity of 34.2 m/sec, a 50 mm thick plate is not perforated according to NDRC penetration prediction, and is therefore safe. It is smaller than the perforation limit thickness according to the Corps of Engineers penetration prediction and is therefore unsafe and is slightly below the perforation limit thickness according to Petry's penetration prediction.

Calculations with the present model yield a maximum penetration depth of 12.6 mm into a semi-infinite target. When the projectile reaches a penetration depth of 9.4 mm the transition between stage I and stage II occurs. The bell-shaped plug is pushed forward at a very low velocity. The negligible residual velocity of the plug indicates a perforation limit at that velocity.

Table 2. SRI tests

V_0 (m/sec)	Target	Measured depth (mm)	Penetration depth prediction (mm)		
			Petry	Corps of Engineers	NDRC
16.7	R.C.	1	3.71	15.24	9.07
22.3	R.C	1.7	6.60	17	11.68
34.2	R.C.	12	17.27	23.11	15.21

Table 3. Calculated perforation limit thickness (mm)

V_0 (m/sec)	Petry			COE			NDRC		
	Eqn (2)	Eqn (4)	Eqn (6)	Eqn (2)	Eqn (4)	Eqn (6)	Eqn (2)	Eqn (4)	Eqn (6)
16.7	7.4	33.6	11.4	30.5	47.9	41.0	18.1	40.3	26.2
22.3	13.2	37.2	19.6	34	50.1	44.8	23.4	43.5	32.8
34.2	34.5	50.4	45.4	46.2	57.7	56.3	30.4	47.9	41.0

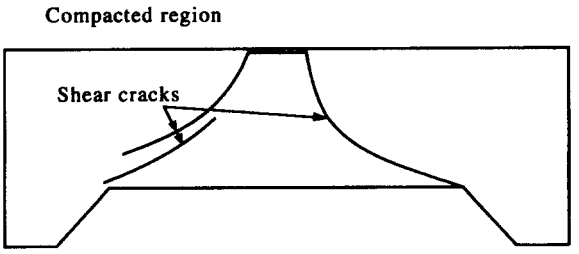

(a) Shear cracks at impact velocity of 22.3 m/sec

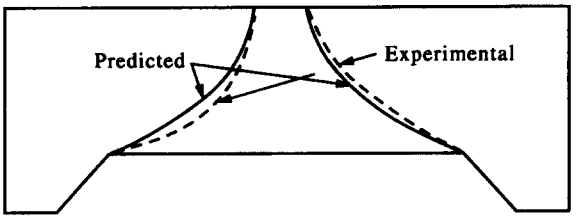

(b) Crater at impact velocity of 34.2 m/sec

Fig. 10. Example 3—comparison of models predictions with SRI test data.

The pattern of shear cracks in the target, at an impact velocity where no significant penetration occurs is shown in Fig. 10, and indicate that failure surfaces which produce the bell-shaped plug already develop at that low velocity. At higher velocities the full plug is formed.

The predicted geometry of the plug is shown in Fig. 10(b) and is found to be in close agreement with the test data.

SUMMARY AND CONCLUSIONS

It is commonly required to provide concrete walls withstanding the effects of low velocity missile impact. Walls of limited thickness may be perforated although their thickness is considerably larger than the same projectile penetration depth in a thick target.

There exist many empirical formulae to account for the penetration into a thick target and for the perforation limit in a thinner target. Their predictions vary considerably and they are not related to physical and mechanical parameters.

The present paper presents a two-stage model which couples a penetration model into a thick target and a punching shear model in a concrete element, earlier developed by the author. The two-stage model enables one to extend the penetration analysis to thin elements and predict whether perforation occurs or not.

The model has been compared with empirical formulae and with test results and has been found to predict the perforation thickness as well as the crater shape and the residual projectile energy.

REFERENCES

1. Kennedy, R. P., A review of procedures for the analysis and design of concretre structures to resist missile impact effects. *Nuclear Engineering and Design*, 1976, **37**, 183–203.
2. Gupta, Y. M. and Seaman, L., Local response of reinforced concrete to missile impact. SRI Report NP-1217, EPRI, 1979.
3. Amirikian, A., Design of protective structures, Report NT-3726, Bureau of Yards and Docks, Department of the Navy, 1950.
4. Haldar, A. and Hamich, H., Local effect of solid missiles on concrete structures. *ASCE, Journal of Structural Engineering*, 1984, **110** (5), 948–960.
5. Kar, A. K., Local effects of tornado generated missiles. *ASCE, Journal of Structural Division*, 1978, **104** (ST5), 809–816.
6. Barr, P., Guidelines for the design and assessment of concrete structures subjected to impact. *AEA*, 1990.
7. Yankelevsky, D. Z. and Adin, M. A., A simplified analytical method for soil penetration analysis. *International Journal for Numerical and Analytical Methods in Geomechanics*, 1980, **4**, 233–254.
8. Yankelevsky, D. Z. and Leibowitz, O., Punching shear in concrete slabs. Submitted for publication, *International Journal of Mechanical Sciences*, 1996.
9. Barr, P., Replica scaling studies of hard missile impacts on reinforced concrete. *Proceedings of the Interassociation Symposium on Concrete Structures Under Impact and Impulsive Loading*, BAM, Berlin 1982, pp. 329–344.